Formins determine the functional properties of actin filaments in yeast.

Matthew Johnson, Daniel A. East[1] and Daniel P. Mulvihill*

School of Biosciences, University of Kent, Canterbury, Kent, CT2 7NJ, UK.

*Author for correspondence e-mail: d.p.mulvihill@kent.ac.uk

Tel: +44 (0) 1227 827239

[1]Current address: Royal Veterinary College, Royal College Street, London, NW1 0TU, UK

Key words: *Schizosaccharomyces pombe*, fission yeast, actin dynamics, Cdc8, For3, Cdc12.

Running Title: Formins modulate Tm recruitment & actin dynamics.

Summary

The actin cytoskeleton executes a broad range of essential functions within a living cell. The dynamic nature of the actin polymer is modulated to facilitate specific cellular processes at discrete locations by actin binding proteins (ABPs) including the formins and tropomyosins (Tm). Formins nucleate actin polymers, while Tms are conserved dimeric proteins that form polymers along the length of actin filaments. Cells possess different Tm isoforms each capable of differentially regulating the dynamic and functional properties of the actin polymer. However the mechanism by which a particular Tm localises to a specific actin polymer is unknown. Here we show that specific formin family members dictate which Tm isoform will associate with a particular actin fialment to modulate their dynamic and functional properties at specific cellular locations. Exchanging the localisation of the fission yeast formins, For3 and Cdc12, resulted in an exchange in localisations of Tm forms on actin polymers. This nucleator driven switch in filament composition was reflected in a switch in actin dynamics, together with a corresponding change in the filament's ability to regulate ABPs and myosin motor activity. These data establish a role for formins in dictating which specific Tm variant will associate with a growing actin filament and therefore specify the functional capacity of the actin filaments which they create.

Highlights

- Describes how formins modulate actin dynamics at specific cellular locations.
- The Formin determines which actin binding proteins associate with actin.
- Formins dictate the Tm composition and functional properties of actin polymers.
- Recruitment of the correct Tm is crucial for proper myosin function.

Results and Discussion

The actin cytoskeleton plays a pivotal role in facilitating growth during the life cycles of eukaryotes. Regulated by accessory proteins, actin polymerises into dynamic filaments, which can bundle to form cables and act as tracks for myosin motors. Actin is nucleated by the Arp2/3 complex and formins, a conserved group of proteins that catalyse the processive addition of actin monomers to the barbed end of the polymer [1]. The dynamic and functional properties of different actin polymers are temporally and spatially regulated to facilitate discrete functions through association with ABPs, including Tm. Tms persist in multiple forms within the cell, each associating with actin at distinct locations to modify the nature of the actin polymers [2-4] to facilitate specific cellular functions [5-9].

Schizosaccharomyces pombe possesses a single Tm, Cdc8 [10], that persists in both amino-terminally acetylated ($_{Ace}Tm^{Cdc8}$) and unacetylated ($_{unace}Tm^{Cdc8}$) forms [11]. Acetylation stabilises Tm^{Cdc8} polymers to promote tight actin binding and regulate myosins. In contrast $_{unace}Tm^{Cdc8}$ filaments form a weaker, more flexible interaction with actin and are unable to regulate actomyosin interactions to the same extent as $_{Ace}Tm^{Cdc8}$ [11, 12]. Each form localises to distinct actin structures within the yeast cell, $_{Ace}Tm^{Cdc8}$ to Cytokinetic Actomyosin Ring (CAR) during mitosis, while $_{unace}Tm^{Cdc8}$ localises to dynamic cytoplasmic actin polymers that extend from the cell tips during interphase [13]. Each actin structure has distinct dynamic properties and is nucleated by different formins: Cdc12 ($Formin^{Cdc12}$) at the CAR during early

mitosis, and For3 (Formin^{For3}) at the growing ends of the cell during interphase.

We asked whether formins regulate actin function by determining the ABP (including Tm) composition of different actin structures? To this end we generated constructs encoding formin-fusion proteins that exchanged the normal distribution of Formin^{For3} and Formin^{Cdc12} [14, 15]. Tea1 is a polarity factor delivered on microtubules to the cell poles, where it is anchored to the membrane by Tea4/Wsh3 [16, 17]. Fusion of Tea1 to the amino terminus of either Formin^{Cdc12} or Formin^{For3} (generating Tea1-Formin^{Cdc12} & Tea1-Formin^{For3}) targeted both formins to the cell poles of wild type, *for3*, *tea1*, and *tea4* deletion cells (Fig. 1A, S1).

The ability of each fusion to nucleate actin was assessed using a GFP actin label (Fig. 1B) and immunostaining all fission yeast Tm^{Cdc8} using an anti-Tm^{Cdc8} antibody (Fig. S1) [11]. This illustrated the presence of interphase actin cables in *for3*Δ *cdc12-112* cells expressing either Tea1-Formin^{For3}, Tea1-Formin^{Cdc12} or the *for3*$^{+}$ gene. In stark contrast antibodies that only detect Tm in its acetylated state [13] gave no signal in the *for3*Δ Tea1-Formin^{For3} cells and staining of interphase actin filaments in the Tea1-Formin^{Cdc12} cells (Fig. 1C, S1). In addition strongly stained arrays of actin-Tm^{Cdc8} cables were often observed in interphase cells expressing Tea1-Cdc12, signifying the composition of the actin bundles is different from normal Formin^{For3} nucleated interphase actin polymers (Fig. 1B, S1). Thus, acetylated Tm only associates with Cdc12 nucleated filaments, indicating that the formin

at the tip of the actin filament either directly or indirectly specifies which Tm is recruited onto the actin polymer

The impact each formin-Tm combination had upon the dynamic nature of actin polymers was assessed using either LifeAct or a calponin homology domain GFP fusion (CHD^{Rng2}) [18, 19] (Fig. 2A, S2, Table 1, Supplemental Movie 1). Growth rates of *for3*Δ cells expressing $Formin^{For3}$ and GFP-CHD^{Rng2} did not differ from wild type when expression from the nmt41 promoter was partially suppressed by adding 4 pmole thiamine. Results were consistent between fluorescent actin markers. Actin filaments nucleated by $Formin^{Cdc12}$ from the cell poles grew 34% faster than those nucleated from $Formin^{For3}$ or in wild type cells (Table 1). This is consistent with *in vitro* studies which indicate formins differentially modulate the rate of actin polymerisation [20]. While filament shrinkage rates were equivalent, mean CHD^{Rng2} fluorescence was 32% higher on polymers nucleated from For3 (Table 1). This observation is consistent with $_{Ace}Tm^{Cdc8}$ filaments sitting in a more stable position on the actin polymer and raising the possibility that the formin and Tm affect the recruitment of the CHD^{Rng2} to actin polymers.

These findings indicate that formins specify which Tm associates with actin to provide a mechanism for modulating the conformation and dynamics of the polymer at discrete cellular locations. The ability of each formin nucleated actin-Tm^{Cdc8} polymer to impact the distribution and activity of ABPs was further tested in the following three ways.

First, by determining whether the different form-actin-Tm^{Cdc8} polymers affected the localisation of cofilin (Adf1/Cof1) and the fission yeast IQGAP

(Rng2). We tested whether the formin and Tm affect cofilin distribution as specific Tm isoforms can recruit cofilin to the actin polymer in mammalian cells [3]. However simultaneous observation of GFP-Adf1 localisation in wild type cells and *for3*Δ *cells expressing* Tea1-Cdc12 revealed modulating the Tm^{Cdc8} composition of pombe actin cables did not affect the distribution of cofilin (Fig. 2B). In contrast, while $IQGAP^{Rng2}$ normally localises to the CAR during mitosis, expressing Tea1-Cdc12 caused the protein to localise to foci at the end of *for3*Δ cells (Fig 2C-D), illustrating formins plays a role in dictating the cellular localisation of the IQGAP.

Second, we examined the impact of each actin-Tm^{Cdc8} complex on the localisation and movement of the yeast myosin V, Myo52. While Myo52-mCherry signal was dispersed throughout the cytoplasm in control *for3*Δ cells, Myo52 foci moved along actin filaments to concentrate at sites of cell growth in *for3*Δ cells expressing either Tea1-For3 or Tea1-Cdc12 formin fusions (Fig. 2E), demonstrating that interphase actin polymers nucleated from each formin fusion can propagate myosin movement. Myo52 moved along Tea1-Cdc12 nucleated interphase actin filaments at 75% the velocity of filaments nucleated by Tea1-For3 (Table 1) or in wild type cells [21] (different at a level of confidence of 99%). While the formin has an impact upon the cellular movement of myosin V within the cell, this may be a consequence of the change in actin polymerization rate it is possible. However the reduction in actin based MyoV motility was reflected in the slower growth rate of Tea1-Cdc12 cells (Table 1).

Third, the ability of each formin to nucleate actin polymers at the CAR was assessed. The carboxyl-terminal half of the myosin II coiled-coil tail alone

localises to the cell equator and CAR in early mitosis [22]. Fusions between the C-terminal half of the Myosin II tail (Myo2T) and either Formin^{For3} or Formin^{Cdc12} were generated (Myo2T-For3 Myo2T-Cdc12, Fig. S3) and their ability to localise to the CAR and complement Formin^{Cdc12} function was monitored in *cdc12-112* cells at 36ºC.

In contrast to *cdc12*Δ cells which lack any medial actin filaments, mitotic *cdc12-112* cells contain randomly organised medial wisps of actin [15] and Myo2 (Fig. S3) at the restrictive temperature. Similarly Myo2 incorporated into disorganised medial filaments in cells expressing Tea1-For3, Tea1-Cdc12 or Myo2T (Fig. 3A). Intriguingly Myo2 associates with filament like structures emanating from the tip of interphase *cdc12-112 tea1-cdc12* cells, indicating the Cdc12 formin can affect the distribution of myosin II within interphase cells. In contrast, Myo2T-Cdc12 and Myo2T-For3 incorporated into a CAR, which contracted with kinetics similar to wild type (Fig. 3B). However, the CAR collapsed in the majority of *cdc12-112* cells expressing Myo2T-For3 upon constriction (Fig 3Av) and cells stopped dividing within 2 divisions (Fig. S3). Immunofluorescence revealed $_{unace}$Tm^{Cdc8}, that associates exclusively with interphase actin polymers and not to the CAR in wild type cells [13], localised to the CAR in the presence of Myo2T-For3 (Fig. 3C, Movie 2), supporting the hypothesis that the formin determines which Tm form associates with the growing actin polymer. These data are consistent with cells lacking acetylated Tm^{Cdc8} frequently forming unstable CARs [13], as only acetylated Tm^{Cdc8} can form the stable polymers that are capable of stabilising actin and regulating myosin II appropriately [13, 23]. Intriguingly, as for Formin^{Cdc12}, For3 dependent actin nucleation is not restricted by location, which suggest that

formins are either constitutively active, their accumulation at a discrete cellular location is sufficient to promote actin polymerisation activity, or that autoinhibition of Cdc12 activity is abolished by amino terminal fusions.

These data demonstrate: (1) formins define the functional properties of the actin filaments they nucleate *in vivo*; (2) formins regulate the Tm isoform that is recruited to the actin polymer and modulate the affinities of other ABPs for the actin polymer; and (3) formins can nucleate functional actin polymers independent of normal cell cycle dependent spatial and temporal constraints.

Cells can express multiple forms of Tm (> 40 isoforms in humans), each localising to a discrete cellular location where they differentially modulate the physical properties of actin polymers to facilitate specific functions [9]. Acetylation provides a level of control additional to variation in sequence to modify the physical properties of Tms and provide a signal to facilitate their recruitment to different actin structures. Formins may modulate the recruitment of associating proteins directly or by modifying conformations in the actin polymer. Formins are not only located at the barbed end of actin filaments where they can associate with the amino termini of the Tm filament incorporating onto the growing actin polymer [24], but also associate with lateral surfaces of the actin filament [25, 26]. Tm can enhance or block ABP binding to actin [8], but Formin may also modulate the pitch of the actin filament directly to change affinities for multiple ABPs [24, 26, 27]. A picture is emerging where formins orchestrate a delicate Tm dependent interplay between ABPs to modulate the functional properties of the actin polymer, allowing actin to facilitate diverse dynamic processes within the cell.

Acknowledgments

We thank Profs F. Chang, I. Hagan and P. Nurse for strains. This work was supported by funding from the Biotechnology and Biological Sciences Research Council (BB/F011784/1 & BB/H016066/1) and a Royal Society Industry Fellowship to DPM.

References

1. Breitsprecher, D., and Goode, B.L. (2013). Formins at a glance. J Cell Sci *126*, 1-7.

2. Creed, S.J., Desouza, M., Bamburg, J.R., Gunning, P., and Stehn, J. (2011). Tropomyosin isoform 3 promotes the formation of filopodia by regulating the recruitment of actin-binding proteins to actin filaments. Exp Cell Res *317*, 249-261.

3. Bryce, N.S., Schevzov, G., Ferguson, V., Percival, J.M., Lin, J.J., Matsumura, F., Bamburg, J.R., Jeffrey, P.L., Hardeman, E.C., Gunning, P., and Weinberger, R.P. (2003). Specification of actin filament function and molecular composition by tropomyosin isoforms. Mol Biol Cell *14*, 1002-1016.

4. Tojkander, S., Gateva, G., Schevzov, G., Hotulainen, P., Naumanen, P., Martin, C., Gunning, P.W., and Lappalainen, P. (2011). A molecular pathway for myosin II recruitment to stress fibers. Curr Biol *21*, 539-550.

5. Ujfalusi, Z., Vig, A., Hild, G., and Nyitrai, M. (2009). Effect of tropomyosin on formin-bound actin filaments. Biophys J *96*, 162-168.

6. Skau, C.T., Neidt, E.M., and Kovar, D.R. (2009). Role of tropomyosin in formin-mediated contractile ring assembly in fission yeast. Mol Biol Cell *20*, 2160-2173.

7. Ujfalusi, Z., Kovacs, M., Nagy, N.T., Barko, S., Hild, G., Lukacs, A., Nyitrai, M., and Bugyi, B. (2012). Myosin and tropomyosin stabilize the conformation of formin-nucleated actin filaments. J Biol Chem *287*, 31894-31904.

8. Wawro, B., Greenfield, N.J., Wear, M.A., Cooper, J.A., Higgs, H.N., and Hitchcock-DeGregori, S.E. (2007). Tropomyosin regulates elongation by formin at the fast-growing end of the actin filament. Biochemistry *46*, 8146-8155.

9. Gunning, P.W., Schevzov, G., Kee, A.J., and Hardeman, E.C. (2005). Tropomyosin isoforms: divining rods for actin cytoskeleton function. Trends Cell Biol *15*, 333-341.

10. Balasubramanian, M.K., Helfman, D.M., and Hemmingsen, S.M. (1992). A new tropomyosin essential for cytokinesis in the fission yeast S. pombe. Nature *360*, 84-87.

11. Skoumpla, K., Coulton, A.T., Lehman, W., Geeves, M.A., and Mulvihill, D.P. (2007). Acetylation regulates tropomyosin function in the fission yeast *Schizosaccharomyces pombe*. J Cell Sci *120*, 1635-1645.

12. East, D.A., Sousa, D., Martin, S.R., Edwards, T.A., Lehman, W., and Mulvihill, D.P. (2011). Altering the stability of the Cdc8 overlap region

modulates the ability of this tropomyosin to bind co-operatively to actin and regulate myosin. Biochem J *438*, 265-273.

13. Coulton, A.T., East, D.A., Galinska-Rakoczy, A., Lehman, W., and Mulvihill, D.P. (2010). The recruitment of acetylated and unacetylated tropomyosin to distinct actin polymers permits the discrete regulation of specific myosins in fission yeast. J Cell Sci *123*, 3235-3243.

14. Feierbach, B., and Chang, F. (2001). Roles of the fission yeast formin for3p in cell polarity, actin cable formation and symmetric cell division. Curr Biol *11*, 1656-1665.

15. Chang, F., Drubin, D., and Nurse, P. (1997). cdc12p, a protein required for cytokinesis in fission yeast, is a component of the cell division ring and interacts with profilin. J Cell Biol *137*, 169-182.

16. Mata, J., and Nurse, P. (1997). tea1 and the microtubular cytoskeleton are important for generating global spatial order within the fission yeast cell. Cell *89*, 939-949.

17. Martin, S.G., McDonald, W.H., Yates, J.R., 3rd, and Chang, F. (2005). Tea4p links microtubule plus ends with the formin for3p in the establishment of cell polarity. Dev Cell *8*, 479-491.

18. Huang, J., Huang, Y., Yu, H., Subramanian, D., Padmanabhan, A., Thadani, R., Tao, Y., Tang, X., Wedlich-Soldner, R., and Balasubramanian, M.K. (2012). Nonmedially assembled F-actin cables incorporate into the actomyosin ring in fission yeast. J Cell Biol *199*, 831-847.

19. Karagiannis, J., Bimbo, A., Rajagopalan, S., Liu, J., and Balasubramanian, M.K. (2005). The nuclear kinase Lsk1p positively regulates the septation initiation network and promotes the successful completion of cytokinesis in response to perturbation of the actomyosin ring in Schizosaccharomyces pombe. Mol Biol Cell *16*, 358-371.

20. Scott, B.J., Neidt, E.M., and Kovar, D.R. (2011). The functionally distinct fission yeast formins have specific actin-assembly properties. Mol Biol Cell *22*, 3826-3839.

21. Grallert, A., Martin-Garcia, R., Bagley, S., and Mulvihill, D.P. (2007). In vivo movement of the type V myosin Myo52 requires dimerisation but is independent of the neck domain. J Cell Sci *120*, 4093-4098.

22. Mulvihill, D.P., Barretto, C., and Hyams, J.S. (2001). Localization of fission yeast type II myosin, Myo2, to the cytokinetic actin ring is regulated by phosphorylation of a C-terminal coiled-coil domain and requires a functional septation initiation network. Mol Biol Cell *12*, 4044-4053.

23. Stark, B.C., Sladewski, T.E., Pollard, L.W., and Lord, M. (2010). Tropomyosin and myosin-II cellular levels promote actomyosin ring assembly in fission yeast. Mol Biol Cell *21*, 989-1000.

24. Galkin, V.E., Orlova, A., Schroder, G.F., and Egelman, E.H. (2010). Structural polymorphism in F-actin. Nat Struct Mol Biol *17*, 1318-1323.

25. Martin, S.G., and Chang, F. (2006). Dynamics of the formin for3p in actin cable assembly. Curr Biol *16*, 1161-1170.

26. Bugyi, B., Papp, G., Hild, G., Lorinczy, D., Nevalainen, E.M., Lappalainen, P., Somogyi, B., and Nyitrai, M. (2006). Formins regulate actin filament flexibility through long range allosteric interactions. J Biol Chem *281*, 10727-10736.

27. Papp, G., Bugyi, B., Ujfalusi, Z., Barko, S., Hild, G., Somogyi, B., and Nyitrai, M. (2006). Conformational changes in actin filaments induced by formin binding to the barbed end. Biophys J *91*, 2564-2572.

Figure Legends

Figure 1. Formins determine dynamics and Tm composition of actin polymers. (A) GFP signal concentrated to the cell poles of *for3*Δ cells either Tea1-GFP (left panels), Tea1-For3-GFP (centre panels) or Tea1-Cdc12-GFP (right panels) fusion proteins. (B) GFP labelled actin structures in *for3*Δ *cdc12-112 gfp-CHD^{rng2}* cells incubated at 36ºC for 4 hours, in which DNA encoding formins or formin fusions had been integrated into the chromosomal *leu1^{+}* locus. Interphase actin cables can only be seen in cells expressing either *for3^{+}, tea1-for3* or *tea1-cdc12*. (C) Anti-acetylated Cdc8 immunofluorescence of wild type (left), *for3*Δ *tea1-for3* (middle) or *for3*Δ *tea1-cdc12* cells revealed $_{ACE}TM^{Cdc8}$ decorated interphase actin filaments (arrows) were only present in cells expressing *tea1-cdc12*. Scales – 5 µm.

Figure 2. Tea1-Cdc12 & Tea1-For3 nucleate functional actin filaments which differentially affect interactions with ABPs. (A) Maximum projections from sub-second timelapse z-stacks illustrate actin polymer dynamics in *for3*Δ *tea1-for3-mCherry* cells. (B) YFP-Cofilin (green) association with cortical actin patches is equivalent in wild type (no cherry signal- marked with asterisks) and *for3*Δ cells expressing Tea1-Cdc12 (magenta). (C&D) YFP-Rng2 localises to (C) the cell poles in *for3*Δ *tea1-for3-mCherry* cells and (D) exclusively to the CAR in wild type cells. (E) Maximum projections of mCherry labelled (magenta) Myo52 in *for3*Δ cells expressing Tea1 (left), Tea1-For3 (middle), or Tea1-Cdc12 (right) GFP carboxyl fusion proteins (green). Myosin V moved along actin polymers in *for3*Δ cells expressing either Tea1-formin fusions, but not in cells expressing Tea1-GFP alone.

Figure 3. A Myo2-tail-For3 fusion recruits to the cell equator and nucleate partially functional contractile rings containing unacetylated Cdc8. (A) mCherry (magenta) and GFP (green) signal in *cdc12-112 myo2-mCherry* cells expressing (i) Myo2T, (ii) Tea1-For3, (iii) Tea1-Cdc12, (iv) Myo2T-Cdc12 or (v) Tea1-Cdc12 GFP fusions, cultured at 36ºC for 4 hrs. While Myo2 associated with Tea1-Cdc12 nucleated interphase actin filaments (iii – arrow), only cells expressing the Myo2T-For3 fusion formed a CAR (iv).

(B) Myo2 rings were seen to constrict within 40 min of forming in all *myo2-mCherry* cells (i) and 5% of *myo2-mCherry cdc12-112* cells expressing Myo2T-For3 (ii) when cultured at 36ºC. (C) Immunofluorescence of wild type (left) and *cdc12-112* (right) cells expressing Myo2T-For3 using anti-Cdc8^{UNACE} antibodies revealed $_{unace}Tm^{Cdc8}$ decorated the medial ring in cells expressing the Myo2T-For3 fusion. Scales – 5 µm.

Table 1. Properties of cells expressing formins and formin fusion

Strain	wild type	*for3Δ for3*	*for3Δ tea1-cdc12*	*cdc12-112 cdc12*	*cdc12-112 myo2T-for3*	*myo2T-cdc12*
% interphase cells with bipolar formin localisation	-	45%	71%	0	0	0
Growth Rate of polar actin filaments[1]	0.57 µmsec^{-1} ± 0.09	0.59 µmsec^{-1} ± 0.10	0.79 µmsec^{-1} ± 0.13	-	-	-
Shrinkage Rate of polar actin filaments[1]	0.77 µmsec^{-1} ± 0.1	0.79 µmsec^{-1} ± 0.17	0.83 µmsec^{-1} ± 0.14	-	-	-
GFP-CHD^{Kng2} intensity on polar actin filaments	nd	141 AU/µm^2	107 AU/µm^2	-	-	-
Mean velocity of myosin V (Myo52)[1]	0.56 µmsec^{-1} ± 0.05	0.59 µmsec^{-1} ± 0.05	0.44 µmsec^{-1} ± 0.01	-	-	-
% mitotic cells with formin localised to contractile CAR	0	0	32%	100%	98%	99
Complement *cdc12-112*	-	-	-	+	-	+
% interphase cells with $_{Ace}Tm^{Cdc8}$-actin cables[2]	0	0	83%	0	0	0
% mitotic cells with $_{unace}Tm^{Cdc8}$ CAR	0	0	0	0	72	0

[1] Determined using methods described in SI. [2] Defined as an interphase cell containing at least one anti-$_{Ace}Tm^{Cdc8}$ antibody labelled cable (see fig S3) n > 200.

Figure 1

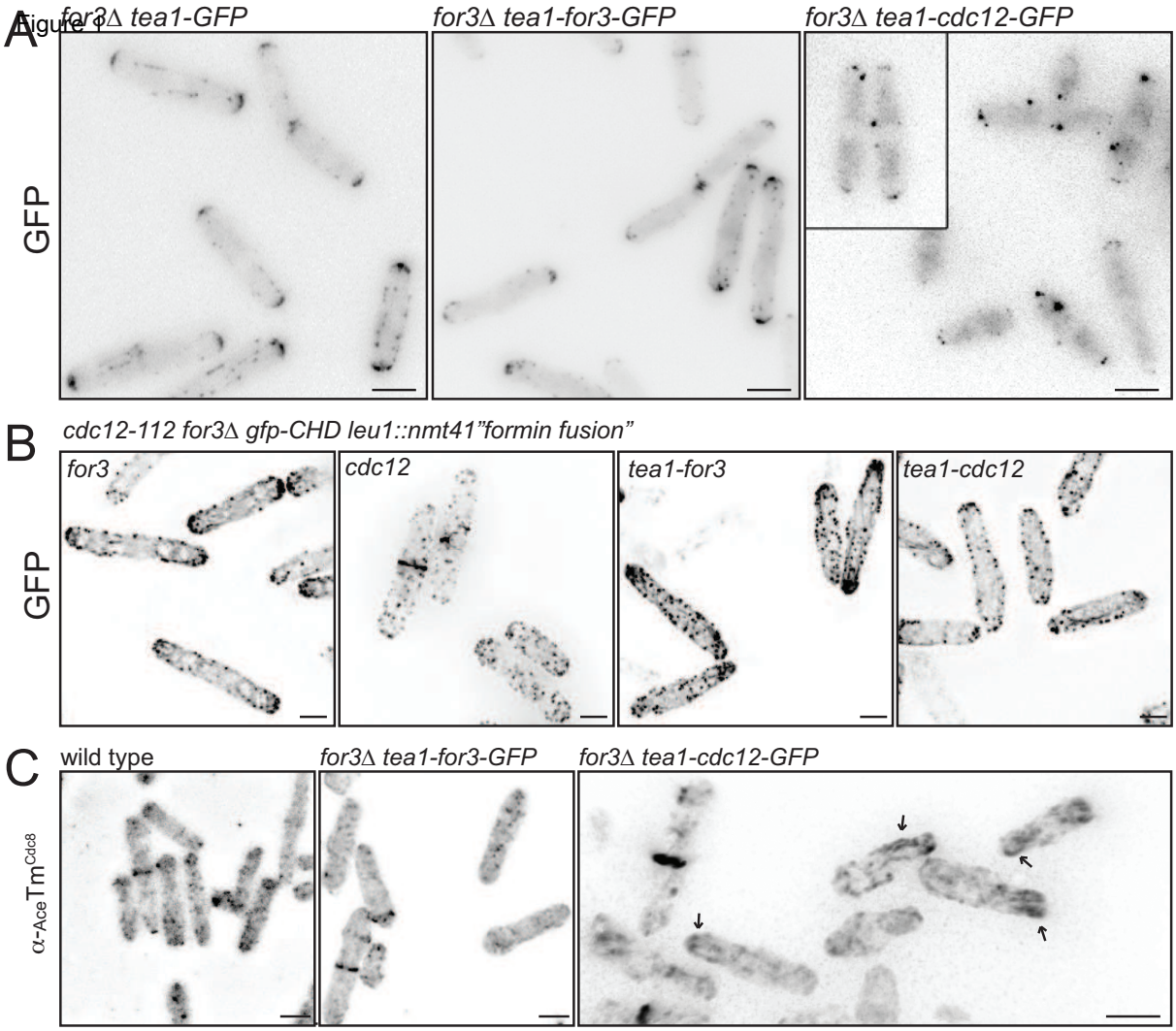

Johnson et al. Figure 1

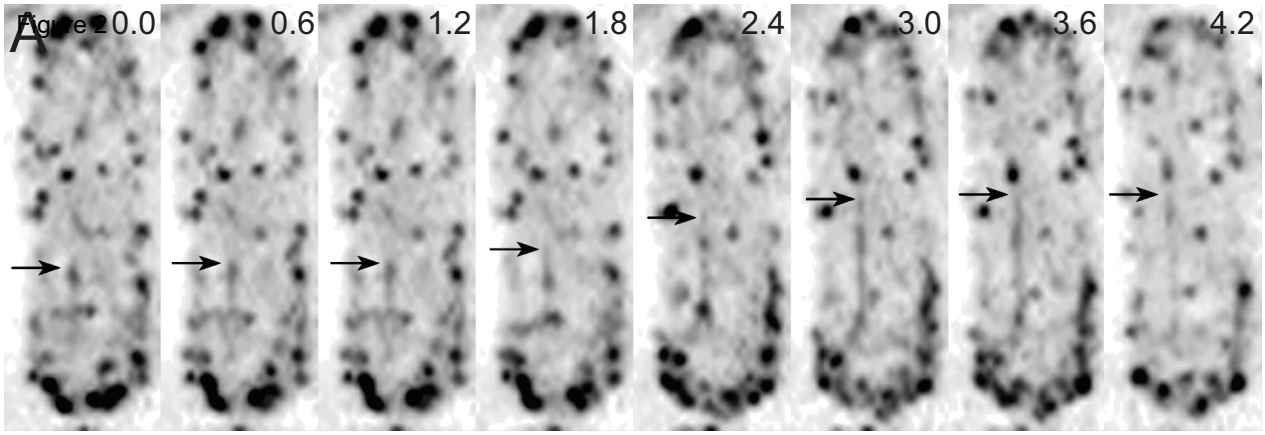

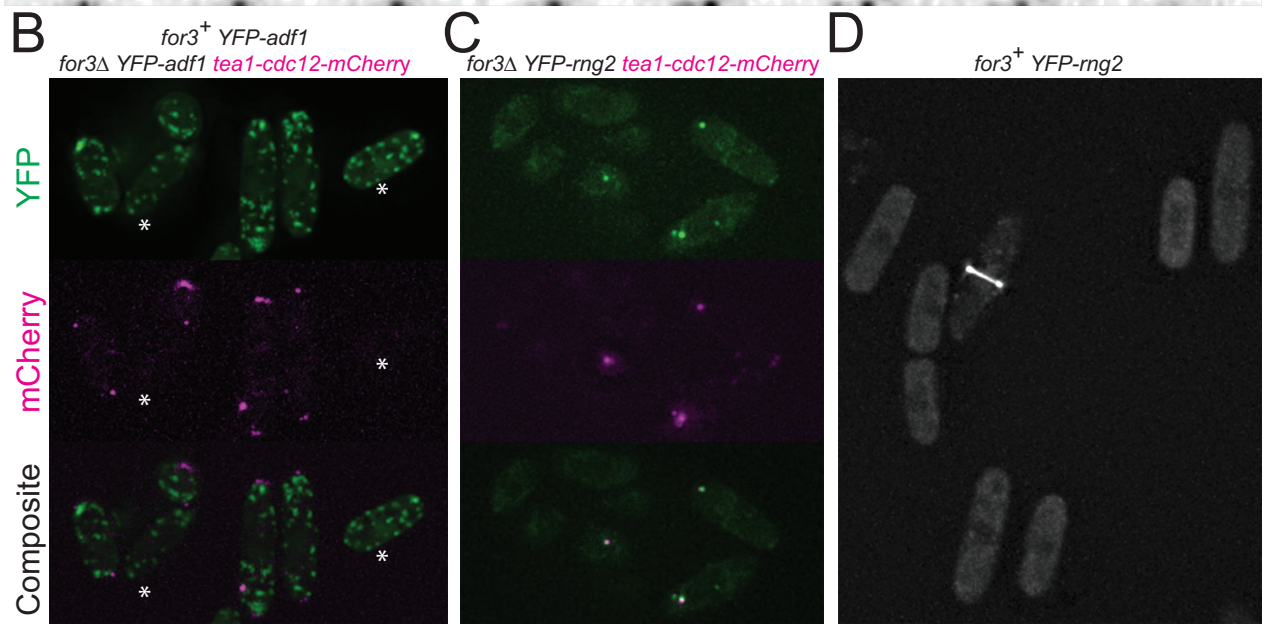

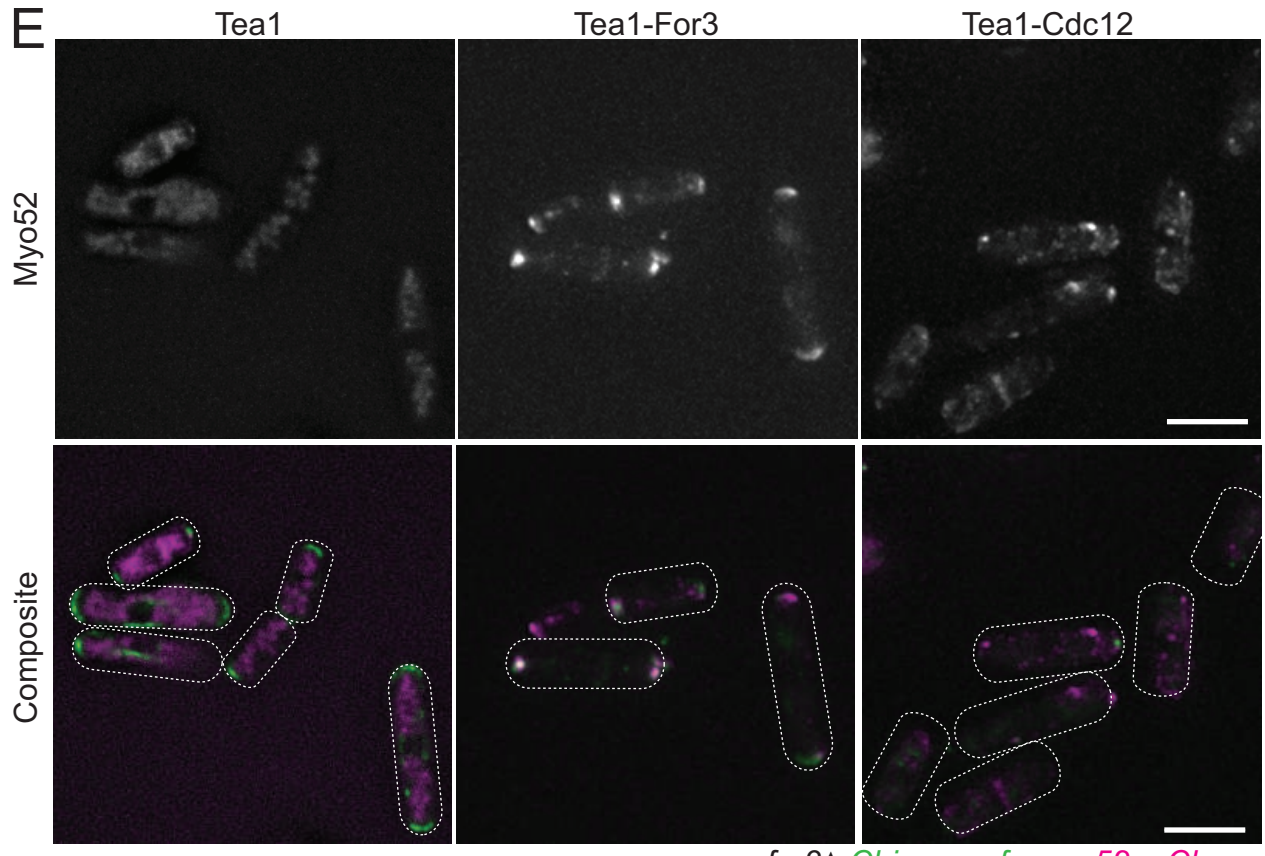

for3Δ Chimera-gfp myo52-mCherry

Johnson et al. Figure 2

Figure 3

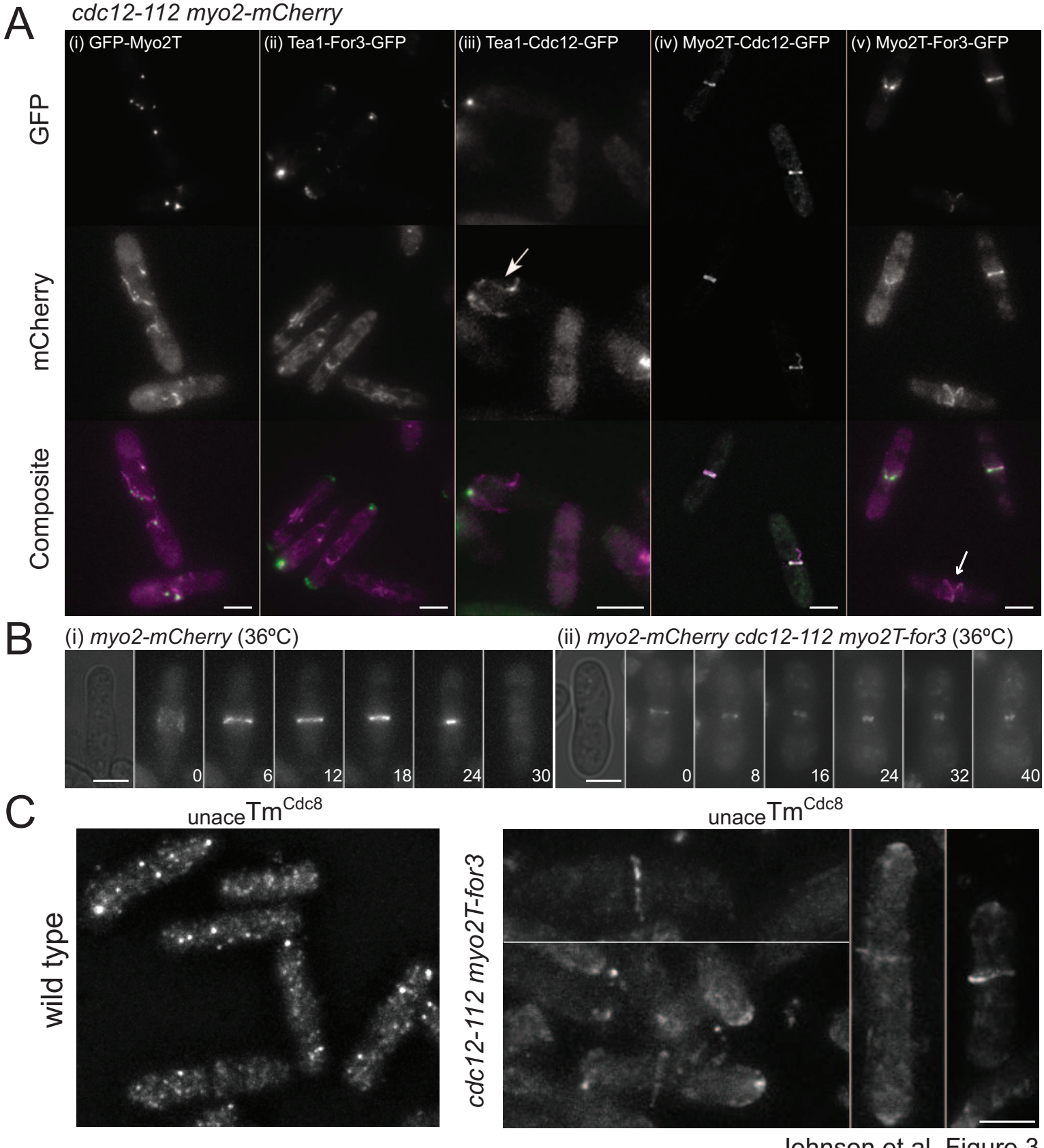

Johnson et al. Figure 3

Supplemental Information

Figure S1

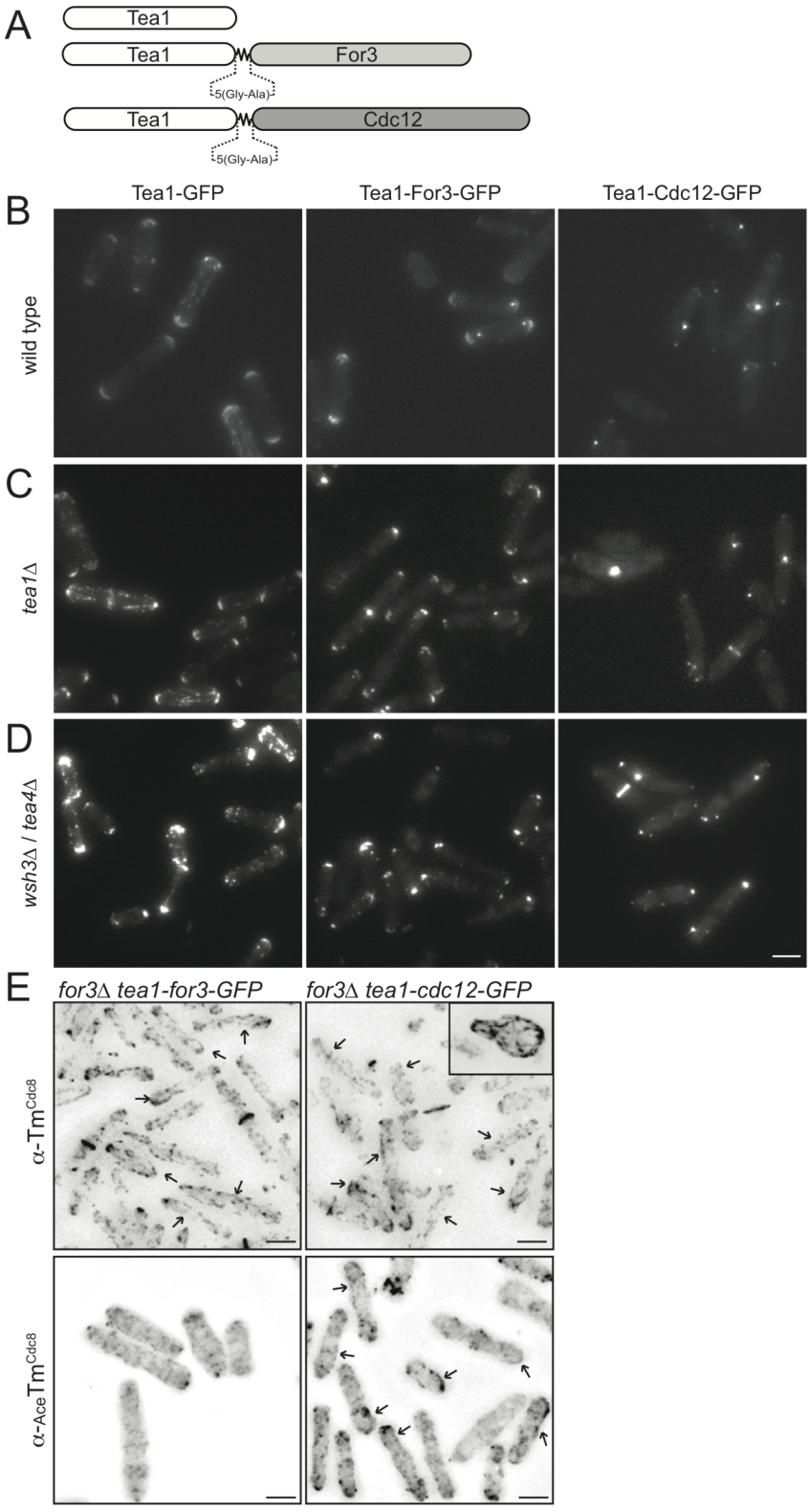

Figure S1 (continued)

F

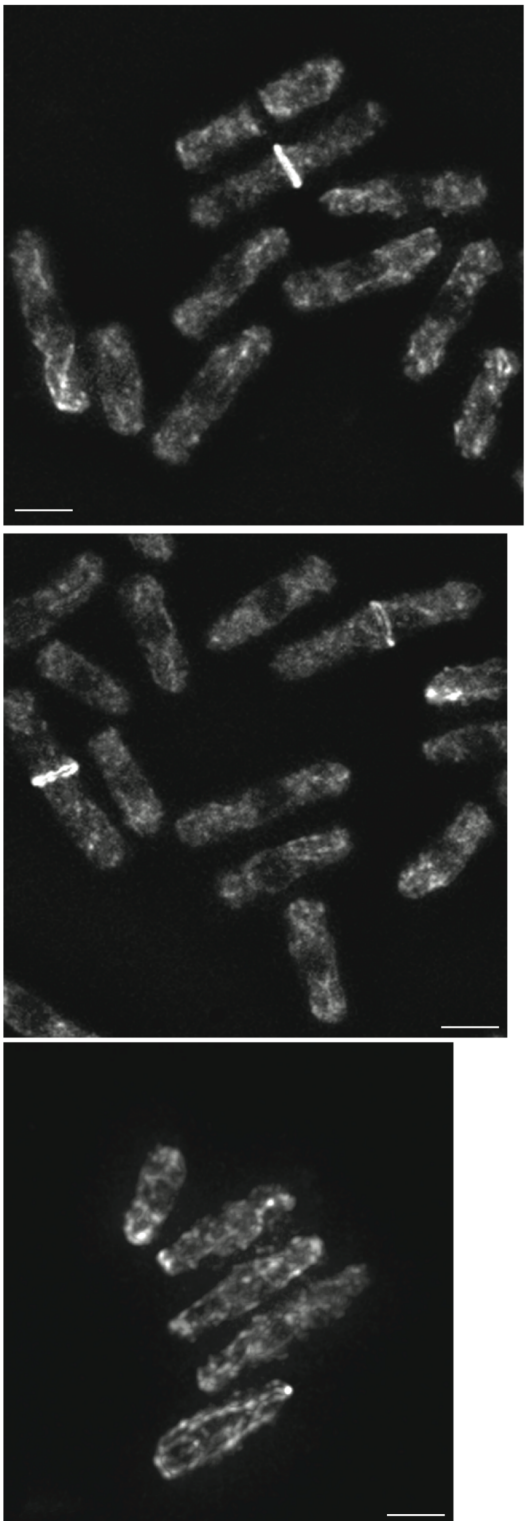

for3Δ tea1-cdc12-GFP
cells subjected to:
α-$_{Ace}$Tm^{Cdc8} immunofluorescence

Figure S2

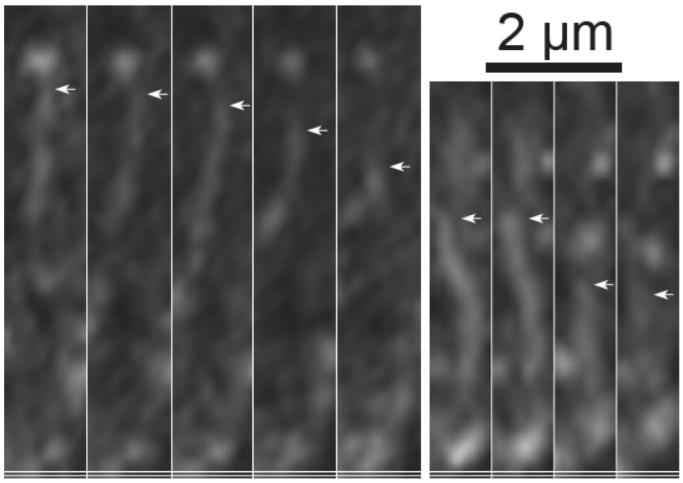

Figure S3

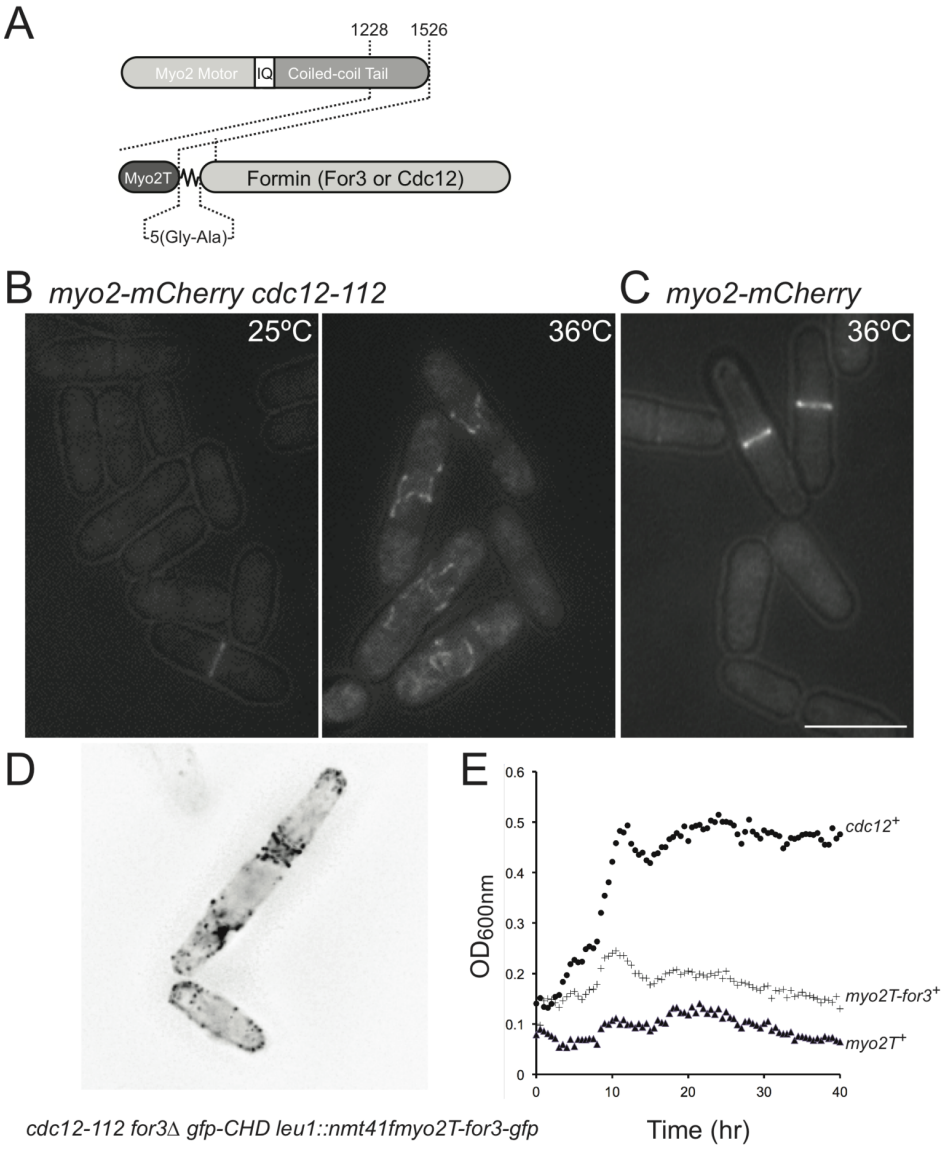
A
1228
1526
Myo2 Motor
IQ
Coiled-coil Tail
Myo2T
Formin (For3 or Cdc12)
5(Gly-Ala)
B myo2-mCherry cdc12-112
25ºC
36ºC
C myo2-mCherry
36ºC
D
E
OD600nm
cdc12+
myo2T-for3+
myo2T+
Time (hr)
cdc12-112 for3Δ gfp-CHD leu1::nmt41fmyo2T-for3-gfp

Supplemental Figure Legends.

Figure S1 (A) Cartoon of Tea1, Tea1-For3 and Tea1-Cdc12 fusion proteins. Micrographs of GFP fluorescence in wild type (B), *tea1*Δ (C), or *wsh3*Δ (D) cells expressing either Tea1-GFP (left panels), Tea1-For3-GFP (middle panels), or Tea1-Cdc12-GFP (right panels) fusion proteins. (E) *for3*Δ cells were cultured expressing either Tea1-For3-GFP (left panels) or Tea1-Cdc12-GFP (right panels) fusion proteins. Cdc8 immunofluorescence (upper panels) revealed actin-Cdc8 filaments (arrows) present only in cells expressing either Tea1-formin fusion. Anti-acetylated Cdc8 antibodies (lower panels) only decorate interphase actin filaments (arrows) in cells expressing Tea1-Cdc12. (F) Example micrographs from independent experiments showing *for3*Δ cells expressing Tea1-Cdc12-GFP which have been subjected to anti-acetylated Cdc8 immunofluorecence. Scales – 5 μm.

Figure S2 Maximum projections from timelapse z-stacks illustrating 2 examples of actin filament shrinkage in *for3*Δ *tea1-for3-mCherry* cells. 1.33 sec/frame. Scales – 2 μm.

Figure S3 (A) Cartoon of Myo2 and Myo2T-Formin (For3 or Cdc12) fusion proteins. mCherry fluorescence-phase composite images of *myo2-mCherry cdc12-112* (B) and *myo2-mCherry* (C) cells cultured at 25ºC or 36ºC. Scale – 10μm. (D) GFP labelled actin structures in *for3*Δ *cdc12-112 gfp-CHD*^{rng2} cells incubated at 36ºC for 4 hours, in which DNA encoding *myo2T-for3* had been integrated into the chromosomal *leu1*$^{+}$ locus. Actin rings can be seen in this strain. (E) Growth curve of *cdc12-112* cells expressing *cdc12* (black circles), *myo2T-for3* (crosses) or *myo2T* (black triangles) cultured in EMM2 at 36ºC.

Supplemental Table 1: *Yeast strains used in this study*

Genotype	Source
ade6-M210 leu1-32 ura4-d18	Lab stock
his2-d1 leu1-32 ura4-d18	Lab stock
for3::kanMX6 ade6-M210 leu1-32 ura4-d18	[S1]
tea1::ura4	[S2]
ura4-d18	Lab stock
tip1-tdTomato:hphMX6 ura4-d18 leu1-32	[S3]
myo52-tdTomato:hphMX6 ura4-d18	[S4]
myo2-mCherry:hphMX6 his3-d1 leu1-32 ura4-d18 ade6-M216	[S4]
myo52-mCherry:hphMX6 ura4-d18	Lab stock
cdc12-112	[S5]
cdc12-112 leu1-32 ura4-d18 his2-d1	Lab stock
myo2-mCherry:hphMX6 for3::kanMX6 leu1-32 ura4-d18	This study
myo52-tdTomato:hphMX6 for3::kanMX6 leu1-32 ura4-d18	This study
cdc12-112 myo2-mCherry:hphMX6 leu1-32 ura4-d18	This study
wsh3::natMX6 leu1-32 ura4-d18 ade6-M210	[S6]
leu1::nmt41for3-mCherry:ura4 ura4.d18	This study
leu1::nmt41tea1-mCherry:ura4 ura4.d18	This study
leu1::nmt41cdc12-mCherry:ura4 ura4.d18	This study
leu1::nmt41tea1-for3-mCherry:ura4 ura4.d18	This study
leu1::nmt41tea1-cdc12-mCherry:ura4 ura4.d18	This study
leu1::nmt41myo2T-for3-mCherry:ura4 ura4.d18	This study
nmt41gfpCHD^{Rng2}:LEU2 leu1-32 ura4-d18	[S7]
pACt1 Lifeact-mCherry:leu1 ade6-m216 leu1-32 ura4-D18	[S8]
ade6-M216 leu1-32 ura4-D18 adf1::[adh-GFP-adf1-ura4^{+}]	[S9]
ura4-Prng2-mYFPx2-rng2 ade6-M210 leu1-32 ura4-D18	[S10]
for3::kanMX6 adf1::[adh-GFP-adf1-ura4^{+}] leu1::nmt41tea1-cdc12-mCherry:ura4 ura4.d18	This study
for3::kanMX6 ura4-Prng2-mYFPx2-rng2 leu1::nmt41tea1-cdc12-mCherry:ura4 ura4.d18	This study
for3::kanMX6 cdc12-112 leu1-32	This study
for3::kanMX6 cdc12-112 nmt41gfpCHD^{Rng2}:LEU2 leu1-32 ura4-d18	This study
for3::kanMX6 cdc12-112 nmt41gfpCHD^{Rng2}:LEU2 leu1::nmt41for3-mCherry:ura4 ura4.d18	This study
for3::kanMX6 cdc12-112 nmt41gfpCHD^{Rng2}:LEU2 leu1::nmt41tea1-for3-mCherry:ura4 ura4.d18	This study
for3::kanMX6 cdc12-112 nmt41gfpCHD^{Rng2}:LEU2 leu1::nmt41tea1-cdc12-mCherry:ura4 ura4.d18	This study
for3::kanMX6 cdc12-112 nmt41gfpCHD^{Rng2}:LEU2 leu1::nmt41cdc12-mCherry:ura4 ura4.d18	This study
for3::kanMX6 cdc12-112 nmt41gfpCHD^{Rng2}:LEU2 leu1::nmt41myo2T-for3-mCherry:ura4 ura4.d18	This study

Supplemental Table 2: *Oligonucleotides used in this study*

#	Name	Sequence (5' to 3')
o363	Tea1-Nde1F	CATATGTCTTTTTTATTTAAAAGG
0364	Tea1-BamH1R	GGATCCATTTTCGTTGTCATGGACTGG
o365	Tea1-$(GA)_3$-Sal1R	GTCGACGGCGCCGGCGCCGGCGCCATTTTCGTTGTCATGGACTGG
o366	For3-Sal1-$(GA)_2$F	GTCGACGGCGCCGGCGCCATGGCATCTAAAATGCCTGAAGGG
o367	For3-BamH1R	GGATCCTTGTTTTTGGCGGTCATTTTCAAC
o368	Cdc12-Xho1-$(GA)_2$F	CTCGAGGGCGCCGGCGCCATGCGAAATTCGTCAAAGGG
o369	Cdc12-BamH1R	GGATCCTTTCTCATTCTCCTTAGGCGCC
o371	Myo2T1228Nde1	CATATGGATCTCTCTAATAAGGTATCGAGTTTGACG
o399	Cdc12-Nde1F	CATATGCGAAATTCGTCAAAGGG
o400	For3-Nde1F	CATATGGCATCTAAAATGCCTGAAGGG

Supplemental Table 3: *Plasmids used in this study*

#	Name	Source
v10	pREP41*cgfp*	[S11]
v474	pREP41*tea1-for3-gfp*	This study
v478	pREP41*tea1-gfp*	This study
v479	pREP41*gfp-myo2T*	[S12]
v490	pREP41*tea1-cdc12-gfp*	This study
v492	pREP41*myo2T-for3-gfp*	This study
v536	pREP41*cdc12-gfp*	This study
v537	pREP41*for3-gfp*	This study
v639	pREP41*myo2T-cdc12-gfp*	This study
v576	pINT41*myo2T-for3-mCherry*	This study
v577	pINT41*tea1-cdc12-mCherry*	This study
v578	pINT41*cdc12-mCherry*	This study
v579	pINT41*tea1-for3-mCherry*	This study
v580	pINT41*for3-mCherry*	This study

Supplemental Experimental Procedures

Yeast cell culture and strains: Cell culture and maintenance were carried out as described elsewhere [S13]. Cells were cultured using Edinburgh minimal media (EMM2) supplemented with amino acids and grown at 25ºC unless stated otherwise. Media was supplemented with 5 μg/ml thiamine to suppress expression from the *nmt41* promoter. Growth rates were determined by generating growth curves using a BMG Spectrostar Nano. Genetic crosses were undertaken on MSA plates [S14]. Strains are listed in Supplemental Table 1.

Molecular Biology: *for3*$^+$ (SPCC895.05), *tea1*$^+$ (SPCC1223.06) and *cdc12*$^+$ (SPAC1F5.04c) genes were amplified from genomic *S. pombe* DNA using appropriate primers (Supplemental Table 2) and cloned into pGEM-T-Easy (Promega). DNA encoding for the carboxyl terminal of the Myo2 coiled-coil tail [S12] was amplified as an *Nde1* – *BamH1* fragment from pREP41GFPMyo2T and cloned into pGEM-T-Easy. The subsequent sequenced genes were cloned into the fission yeast carboxyl-terminal tagging vectors pREP41cGFP [S11] and pINT41cmCherry (lab stock) to generate the appropriate Tea1, formin and chimera constructs (Supplemental Table 3). The latter were designed to include a $(Gly\text{-}Ala)_5$ linker between the targeting polypeptide (i.e. Tea1 or Myo2T) and formin, identical to the Tea1-For3 protein described previously [S15]. pINT plasmids were integrated into the *leu1* locus of *S. pombe* chromosome 1.

Microscopy: Samples were visualized using an Olympus IX71 microscope with PlanApo 100x OTIRFM-SP 1.45 NA lens mounted on a PIFOC *z*-axis focus drive (Physik Instrumente, Karlsruhe, Germany), and illuminated using LED light sources (Cairn Research Ltd, Faversham, UK) with appropriate filters (Chroma, Bellows Falls, VT). An Optosplit device (Cairn Research Ltd) was used to allow simultaneous acquisition of signals from two fluorophores that emitted light of different wavelengths. Samples were visualized using either a QuantEM (Photometrics) or ProEM 1024B (Princeton Instruments) EMCCD camera, and the system was controlled with Metamorph software (Molecular Devices). Each 3D-maximum projection of volume data was

calculated from 31 *z*-plane images, each 0.2 µm apart, using Metamorph or Autoquant X software. During live-cell imaging, cells were mounted onto coverslips with lectin (Sigma L2380; 1 mg/ml) in a Bioptechs FCS2 (Bioptechs, Butler, PA), fitted onto an ASI motorized stage (ASI, Eugene, OR) on the above system, with the sample holder, objective lens and environmental chamber held at the required temperature. All live-cell imaging was undertaken using EMM2 media supplemented with appropriate amino acids. Indirect immunofluorescence microscopy was performed as described previously [S16] except that glutaraldehyde was omitted. Anti-Cdc8 sera [S17] were used at a dilution of 1:100 while anti-Cdc8^{ACE} and anti-Cdc8^{UNACE} acetylation state specific antibodies [S4] were used at a dilution of 1:50 and 1:2 respectively. More than 300 cells / sample were counted to determine localisation statistics, while over 1000 cells / sample were measured for calculating mean cell lengths. Mean myosin V velocities were calculated by fitting velocities of more than 300 foci movements to a Gaussian distribution.

Image preparation: Images were processed using Adobe Photoshop software. Adjustments in contrast and brightness were equivalent for all cell types within the same experiment (as per journal guidelines). Images within Figures 1, 2 and S1 were inverted to highlight actin filaments. Figures were prepared using Adobe Illustrator.

Analysis of filament dynamics: Growth and shrinkage of actin filaments was measured using Metamorph software. Timelapse movies of 13 x 0.2 µm z-slice time frames (0.667 sec / time point; 200 time points,) were acquired and analysed in a frame-by-frame manner, looking for actin filament growth from the cell poles. Care was taken to ensure that only growth events of a filament nucleating from a single point at the cell poles were measured. This was to ensure that measurements in filament length were not affected by flux, movement or bending. The difference in filament length and time taken were recorded, and rate of filament growth/shrinkage was then calculated. At least 30 growth and shrinkage events were measured for each strain. Examples of frames from a timelapse of two filament shrinkage events are shown in Figure S3A.

References

S1. Feierbach, B., and Chang, F. (2001). Roles of the fission yeast formin for3p in cell polarity, actin cable formation and symmetric cell division. Curr Biol *11*, 1656-1665.

S2. Mata, J., and Nurse, P. (1997). tea1 and the microtubular cytoskeleton are important for generating global spatial order within the fission yeast cell. Cell *89*, 939-949.

S3. Martin-Garcia, R., and Mulvihill, D.P. (2009). Myosin V spatially regulates microtubule dynamics and promotes the ubiquitin-dependent degradation of the fission yeast CLIP-170 homologue, Tip1. J. Cell Sci. *122*, 3862-3872.

S4. Coulton, A.T., East, D.A., Galinska-Rakoczy, A., Lehman, W., and Mulvihill, D.P. (2010). The recruitment of acetylated and unacetylated tropomyosin to distinct actin polymers permits the discrete regulation of specific myosins in fission yeast. J Cell Sci *123*, 3235-3243.

S5. Nurse, P., Thuriaux, P., and Nasmyth, K. (1976). Genetic control of the cell division cycle in the fission yeast Schizosaccharomyces pombe. Mol Gen Genet *146*, 167-178.

S6. Alvarez-Tabares, I., Grallert, A., Ortiz, J.M., and Hagan, I.M. (2007). Schizosaccharomyces pombe protein phosphatase 1 in mitosis, endocytosis and a partnership with Wsh3/Tea4 to control polarised growth. J Cell Sci *120*, 3589-3601.

S7. Karagiannis, J., Bimbo, A., Rajagopalan, S., Liu, J., and Balasubramanian, M.K. (2005). The nuclear kinase Lsk1p positively regulates the septation initiation network and promotes the successful completion of cytokinesis in response to perturbation of the actomyosin ring in Schizosaccharomyces pombe. Mol Biol Cell *16*, 358-371.

S8. Huang, J., Huang, Y., Yu, H., Subramanian, D., Padmanabhan, A., Thadani, R., Tao, Y., Tang, X., Wedlich-Soldner, R., and Balasubramanian, M.K. (2012). Nonmedially assembled F-actin cables incorporate into the actomyosin ring in fission yeast. J Cell Biol *199*, 831-847.

S9. Nakano, K., and Mabuchi, I. (2006). Actin-depolymerizing Protein Adf1 Is Required for Formation and Maintenance of the Contractile Ring during Cytokinesis in Fission Yeast. Mol Biol Cell *17*, 1933-1945.

S10. Takaine, M., Numata, O., and Nakano, K. (2009). Fission yeast IQGAP arranges actin filaments into the cytokinetic contractile ring. Embo J *28*, 3117-3131.

S11. Craven, R.A., Griffiths, D.J., Sheldrick, K.S., Randall, R.E., Hagan, I.M., and Carr, A.M. (1998). Vectors for the expression of tagged proteins in Schizosaccharomyces pombe. Gene *221*, 59-68.

S12. Mulvihill, D.P., Barretto, C., and Hyams, J.S. (2001). Localization of fission yeast type II myosin, Myo2, to the cytokinetic actin ring is regulated by phosphorylation of a C-terminal coiled-coil domain and requires a functional septation initiation network. Mol Biol Cell *12*, 4044-4053.

S13. Moreno, S., Klar, A., and Nurse, P. (1991). Molecular genetic analysis of fission yeast Schizosaccharomyces pombe. Methods Enzymol *194*, 795-823.

S14. Egel, R., Willer, M., Kjaerulff, S., Davey, J., and Nielsen, O. (1994). Assessment of pheromone production and response in fission yeast by a halo test of induced sporulation. Yeast *10*, 1347-1354.

S15. Martin, S.G., McDonald, W.H., Yates, J.R., 3rd, and Chang, F. (2005). Tea4p links microtubule plus ends with the formin for3p in the establishment of cell polarity. Dev Cell *8*, 479-491.

S16. Hagan, I.M., and Hyams, J.S. (1988). The use of cell division cycle mutants to investigate the control of microtubule distribution in the fission yeast Schizosaccharomyces pombe. J Cell Sci *89 (Pt 3)*, 343-357.

S17. Skoumpla, K., Coulton, A.T., Lehman, W., Geeves, M.A., and Mulvihill, D.P. (2007). Acetylation regulates tropomyosin function in the fission yeast *Schizosaccharomyces pombe*. J Cell Sci *120*, 1635-1645.

Supplemental Movie 1 Time lapse of GFP fluorescence 13 z slice maximum projections of *for3Δ leu1::nmt41for3*$^{+}$ *gfp-CHD* cells cultured at 25ºC in EMM2. 666 mec / frame.

Supplemental Movie 2 Rotation of fluorescence from *cdc12-112 myo2T-for3* cell, cultured 36ºC for 4 hours and subjected to subsequent anti-Cdc8^{UNACE} immunofluorescence.

Supplemental Movie 1
Click here to download Supplemental Movie and Spreadsheet: Johnson et al Movie S1.mov

Supplemental Movie 2
Click here to download Supplemental Movie and Spreadsheet: Johnson et al Movie S2.mov